Cell Reports
Physical Science

CellPress
OPEN ACCESS

Perspective

Computational flow visualization to reveal hidden properties of complex flow with optical and computational methods

Jianqing Huang,[1,2,4,5] Hecong Liu,[3,5,*] Shuo Zhu,[2] Yingzheng Liu,[1] Edmund Y. Lam,[2,*] and Weiwei Cai[1,*]

SUMMARY

Flow visualization has long played a crucial role in understanding complex fluid dynamics, especially reactive flows, but traditional techniques face limitations in realizing the measurement of multiple dimensionality and multiple physical parameters. In this perspective, we introduce computational flow visualization, a new paradigm that combines optical and computational methods to revolutionize experimental flow analysis. We showcase representative techniques that excel in multi-dimensional and multi-parameter measurements, enabling detailed insights into flow phenomena. To address key challenges, such as spatial resolution, computational efficiency, harsh environments, and portability, we emphasize the immense opportunities offered by advanced reconstruction algorithms, novel imaging modalities, and cutting-edge optical components. By leveraging these advancements, computational flow visualization promises more accurate, higher-dimensional, real-time, and intelligent assessments across diverse applications. This transformative approach unlocks new frontiers in our understanding of intricate flow characteristics, with implications spanning from fundamental fluid dynamics research to practical fields like engineering, environmental monitoring, and biomedical research.

INTRODUCTION

Flow visualization techniques are integral to fluid-related disciplines such as fluid dynamics, aerodynamics, combustion science, and chemical engineering, offering means to illustrate and understand the patterns and dynamics of fluid flow.[1] These methodologies are particularly valuable given the inherent transparency of fluids, enabling researchers and engineers to extract both quantitative and qualitative data regarding flow characteristics, such as velocity, pressure, temperature, and density fields. For reactive flows, the visualization of species is another important topic. Merzkirch[2] categorized flow visualization techniques into three primary types: introducing foreign materials into gas or liquid flows (e.g., particle image velocimetry [PIV][3]), employing optical methods based on density variation (e.g., interferometry,[4] Schlieren and shadowgraphy[5]), and marking flow fields through the addition of heat or energy (e.g., laser-induced fluorescence [LIF][6]). These techniques provide invaluable insights into phenomena like turbulence, vortex separation, and shock waves, thereby facilitating the design and optimization of various systems and processes. These optically based methods have the advantages of non-intrusiveness and fast responses. Even within the first category, where foreign materials are introduced into the flow, optical detectors are essential for capturing the motion of these

[1]Key Lab of Education Ministry for Power Machinery and Engineering, School of Mechanical Engineering, Shanghai Jiao Tong University, 800 Dongchuan Road, Shanghai, China

[2]Department of Electrical and Electronic Engineering, The University of Hong Kong, Pokfulam, Hong Kong SAR, China

[3]EMPI, Institute for Energy and Materials Processes-Reactive Fluids, University of Duisburg-Essen, 47048 Duisburg, Germany

[4]School of Aerospace Engineering, Xiamen University, Xiang'an South Road, Xiang'an District, Xiamen 361005, Fujian, China

[5]These authors contributed equally

*Correspondence: hecong.liu@uni-due.de (H.L.), elam@eee.hku.hk (E.Y.L.), cweiwei@sjtu.edu.cn (W.C.)

https://doi.org/10.1016/j.xcrp.2024.102282

This is an open access article under the CC BY-NC license (http://creativecommons.org/licenses/by-nc/4.0/).

materials, and the added materials should not change the nature of the flow. However, as most practical industrial flows are physically and geometrically complex, such traditional flow visualization techniques have their own limitations, which may include restrictions in multiple dimensionality and multi-parameter coupling. For example, planar LIF can only measure two-dimensional (2D) quantities, lacking volumetric resolution, and coherent anti-Stokes Raman spectroscopy is limited by temperature and pressure coupling.

Computational optical imaging stands as an increasingly promising paradigm that exploits advancements in computational resources.[7,8] Its key distinction from traditional imaging lies in the incorporation of imaging models, which provide specific physical interpretations. Unlike traditional methods that directly produce images as representations of the scene or object, computational optical imaging employs additional computational algorithms to extract hidden or higher-dimensional optical information (e.g., phase, polarization, spectrum), which may not be readily observable in raw images.[9,10] These techniques also enable the enhancement of specific aspects of the captured images, including resolution, and the revelation of hidden details. The post-processing techniques employed in computational optical imaging encompass a wide range of methods, with reconstruction algorithms being the most important. Nevertheless, computational optical imaging also faces a significant challenge compared to traditional imaging, i.e., computational efficiency. The advancement of computational optical imaging has spurred the emergence of numerous novel imaging technologies, including lensless imaging,[11] scattering imaging,[12] polarization imaging,[13] and quantum imaging.[14] These innovative approaches have found applications across diverse fields, ranging from machine vision and remote sensing to fluid dynamics, facilitating new insights and advancements in these domains.

The integration of computational optical imaging into flow visualization has catalyzed the emergence of a revolutionary diagnostic approach known as computational flow visualization (CFV). This method leverages comprehensive computational algorithms alongside advanced optical imaging techniques to capture and analyze flow patterns and dynamics, revealing more hidden fluid properties and characteristics. CFV offers notable advantages over traditional methods, including 3D resolution and the ability to measure multiple parameters simultaneously. Currently, three prominent techniques have emerged within CFV: tomography,[15] plenoptic imaging,[16] and digital holography.[17,18] Tomography utilizes multiple projections to augment the dimensionality of measured quantities, plenoptic imaging employs a micro-lens array to split the light, and digital holography enables the extraction of 3D particle information from a single hologram with flexible refocusing capability.[19] In this perspective, we provide an overview of these representative techniques, highlighting the improvement of these techniques and the key challenges and opportunities of CFV. Moreover, we delineate future research directions and discuss the broader implications of CFV.

COMPUTATIONAL FLOW VISUALIZATION

The fundamental concept underlying CFV pertains to the substantial requirements for computational resources. The captured raw images cannot directly represent the nature of flow or just provide limited information. Specific computational approaches are able to reveal more hidden properties of flow by interpreting the captured optical information in different dimensions. This section summarizes the basic concepts of three kinds of widely employed CFV techniques: tomography,

Table 1. Summary for existing computational flow visualization techniques

Techniques	Modalities	Applications
Tomography	emission tomography	velocity, temperature, etc.
Tomography	absorption tomography	temperature, concentration, etc.
Tomography	background-oriented Schlieren tomography	refractive index, density, and temperature
Plenoptic imaging	plenoptic particle image velocimetry	velocity
Plenoptic imaging	plenoptic background-oriented Schlieren	refractive index, density, and temperature
Holography	digital holography	particle size, location, and morphology

plenoptic imaging, and digital holography, which are detailed in Table 1. All techniques can work separately to realize multi-dimensional visualization or be incorporated with each other to implement multi-dimensional, multi-parameter visualization.

Imaging models

Typically, imaging models relate unknown quantities of interest (*QoI*s) and known measurements and can be represented by a mathematical formula, such as $y = f(QoI)+\epsilon$, where y denotes the measurements, which are raw or pre-processed images captured by the optical system, $f(QoI)$ is the mapping function of the unknown variable QoI, and ϵ represents the noises or errors. Distinct CFV techniques employ various imaging models (Figures 1A–1C).

Tomography stands out as one of the most well-known methods, further categorized into emission tomography, laser absorption tomography, and background-oriented Schlieren (BOS) tomography. A traditional tomographic system utilizes multiple sensors to capture images from various directions, and each sensor consists of numerous pixels. In cases where only a single sensor is available, the acquisition of multiple images can be achieved through the rotation of either the sensor or the target,[20] relying on the assumption of temporal stability. Irrespective of the specific tomography type, the measurements are also known as projections, and the mapping function can be further simplified, i.e., $f(QoI) = A \times QoI$, where A is called as the weight matrix. Various factors, such as absorption and scattering of the medium and the arrangement of the tomographic system, can influence the weight matrix and should be taken into consideration when constructing the matrix. The major improvement of tomography to traditional flow visualization is that this technique allows for a 3D visualization of the target flow, thus extending the dimensionality with the cost of resolution due to the limitation of computational resources.

In emission tomography, the projections are line-of-sight integrated emission intensities captured by cameras, and two approaches can be employed to construct the weight matrix: pixel-centric and voxel-centric models (Figure 1A).[15] In the pixel-centric model, each pixel emits a ray interacting with voxels, and the matrix elements represent these intersects. The nature of these intersects depends on the type of rays chosen, such as thin, cylindrical, or conical rays. Parameters like chord length, cylindrical volume, conical volume, or other empirically derived estimations can be used to describe these interactions.[21] In the voxel-centric model, multiple points are assumed within each voxel, and the matrix element is the ratio between the number of received points by a specific pixel and the total points in one voxel.[22] Emission tomography encompasses various tomographic modalities: chemiluminescence,[23] incandescence,[24] scattering,[25] LIF,[26] and laser-induced incandescence.[27] Scattering tomography, for instance, can be employed to infer the velocity field via further

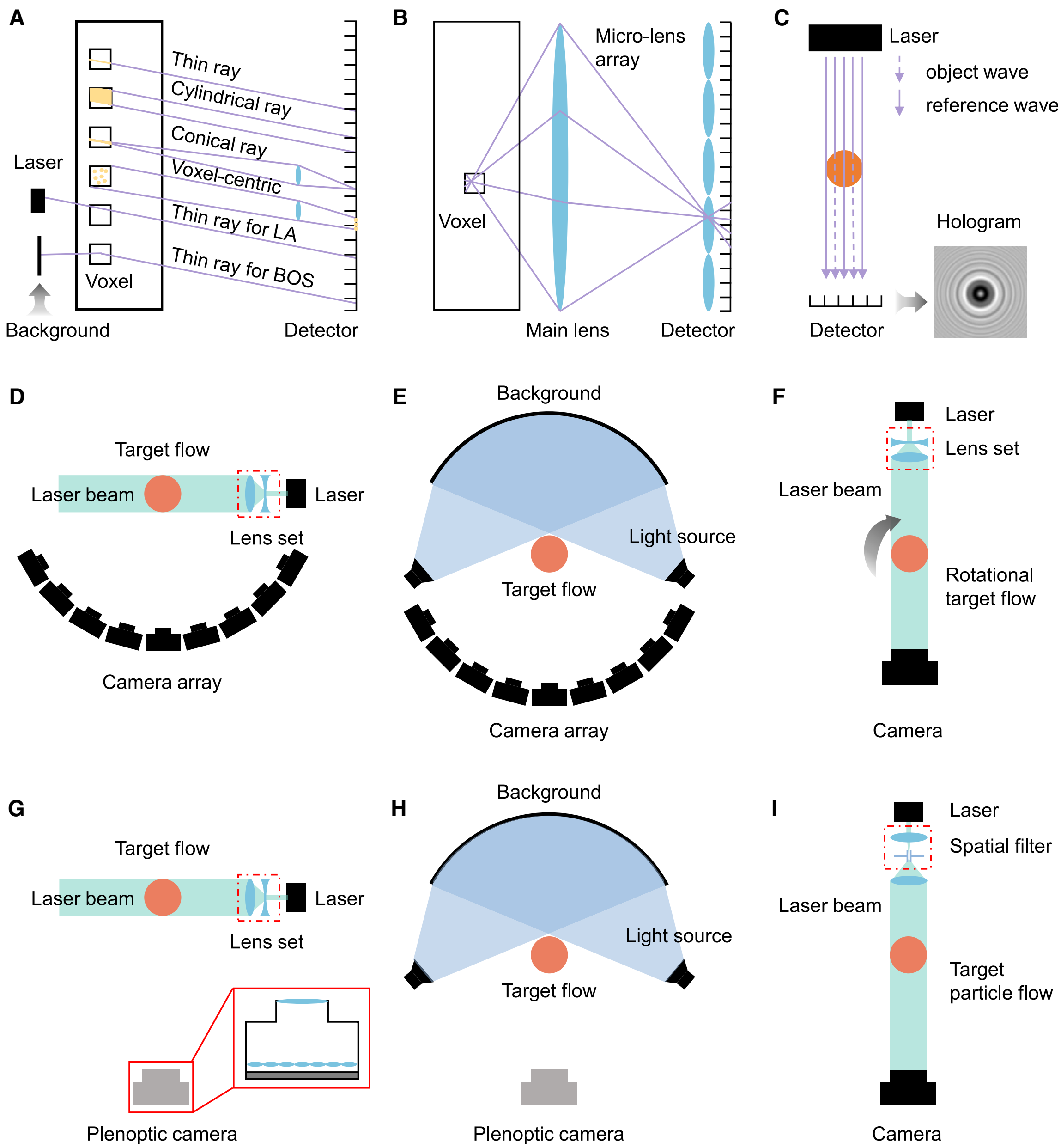

Figure 1. Illustrations of imaging model and flow visualization setup
(A) Imaging model for tomography.
(B) Imaging model for plenoptic imaging.
(C) Imaging model for digital holography.
(D) Flow visualization setup for emission tomography.
(E) Flow visualization setup for background-oriented Schlieren (BOS) tomography.
(F) Flow visualization setup for laser absorption (LA) tomography.
(G) Flow visualization setup for plenoptic imaging.
(H) Flow visualization setup for plenoptic BOS.
(I) Flow visualization setup for digital holography.

correlation[25] or optical flow algorithms,[28] while incandescence serves as a valuable indicator for estimating the temperature field.[29] These modalities leverage distinct physical mechanisms associated with the emission process to provide valuable insights into specific flow characteristics.

In laser absorption tomography, the thin ray model is consistently employed, given that the captured signal is from an external light source.[30] The matrix element is chord length, and the unknown *QoI* is the local absorption coefficient. The projection in this context is represented by the absorbance ($\alpha_v = -\ln(I_{v,0}/I_{v,L})$), where $I_{v,0}$ and $I_{v,L}$ correspond to the light intensity at emitters and sensors, respectively. BOS tomography also uses the thin ray model.[31] The light from the background will be continuously deviated from a straight line due to the different refractive index of the target flow field. As a result, the matrix element is a combination of the chord length and corresponding differential within each voxel, and the unknown *QoI* is the local refractive index.[32] The projection is integrated deflection, which can be calculated from a pair of images (i.e., one with a target flow field and the other without a target flow field). Once the refractive index of the target flow is obtained, the temperature and density can be resolved simultaneously.

Plenoptic imaging, also known as light-field imaging, represents an advanced alternative to tomography, particularly when optical accessibility is limited.[16] Compared to tomographic systems, plenoptic imaging systems are more compact, but this comes at the cost of reduced depth resolution. In plenoptic imaging, a micro-lens array will be installed in front of the sensor to separate the light from different directions. Normally, the light field can be parameterized within a camera by considering two planes of importance. Therefore, the radiance intensity distribution of the light rays can be described by the following 4D plenoptic function, $L = L(u,v,s,t)$, where L is the radiance density and (u,v) and (s,t) are the coordinates of the intersection points between the light ray and the planes.[33] Considering the special design of the plenoptic camera and the fact that one point in space corresponds to multiple points in the sensor plane, the thin ray model is most widely used to construct the weight matrix (Figure 1B). Analogous to tomography, plenoptic imaging encompasses diverse modalities, such as plenoptic BOS and plenoptic PIV. Consequently, the projections and *QoI*s in the imaging model vary across different modalities.

Differing from tomography and plenoptic imaging, the measurements of digital holography (Figure 1C) are hologram, and the mapping function hinges on the interference phenomenon between an object wave (E_O) and a reference wave (E_R).[18] Central to digital holography is the elucidation of this interference pattern to discern and retrieve particle properties,[17] i.e., particle morphology and 3D location. Normally, the object wave is the light diffracted by the particles in the flow field; the reference wave is the illumination light without disturbance from the particles. Following interference, the recorded hologram can be obtained as $I(x,y) = |E_O(x,y) + E_R(x,y)|$,[2] where I is the recorded intensity and (x,y) is corresponding coordinate. The hologram amplitude $h(x,y)$ is proportional to the hologram intensity $I(x,y)$. Both amplitude and phase distributions[34] of the propagating object wavefront are encoded in the holographic fringes, enabling access to the complex light field with proper reconstruction methods.

Reconstruction methods

In mathematical parlance, two types of fundamental problems emerge: the forward problem and the inverse problem.[35] The former entails the utilization of known parameters, often denoted as inputs, in conjunction with a prescribed mapping function to derive resultant projections or outputs. Conversely, the inverse problem involves the utilization of measured outputs, typically in the form of projections, alongside the same mapping function to ascertain the unknown inputs or *QoI*s. While the establishment of the mapping function is usually straightforward, the inversion of said function poses considerable challenges, thereby rendering the inverse problem inherently more complex. This complexity primarily stems from issues such as non-uniqueness, ill-posedness, and noise within the system, which complicate the precise reconstruction of the original inputs from the provided outputs.[15] In CFV methodologies, exemplified by techniques like tomographic reconstruction in fields such as medical imaging and fluid dynamics, the inverse problem is a characteristic challenge and can be solved by iterative methods or cast into a minimization problem, i.e., $QoI = \mathrm{argmin}(\|y - f(QoI)\|)$. Researchers have developed specialized reconstruction methods to address this challenge, aiming to accurately recover the underlying parameters from the measured projections.

The initial method is model-based reconstruction, which necessitates a pre-calculated imaging model. In the realm of tomography, reconstruction can be accomplished through analytic and algebraic algorithms. Analytic algorithms encompass filtered back projection and Abel inversion. Filtered back projection necessitates a substantial quantity of projections,[36] whereas Abel inversion mandates axisymmetric flow,[37] thereby limiting the applicability of both algorithms in practical flow visualization. In algebraic algorithms, the *QoI* is reconstructed using iterative methods with an initial guess. Two distinct approaches exist within algebraic methods. The first approach involves updating individual *QoI* values one by one during each iteration, e.g., the algebraic reconstruction technique (ART),[38] multiplicative ART,[39] and maximum likelihood expectation maximization.[40] In contrast, the second approach involves updating all *QoI* values simultaneously and comprehensively within each iteration, resulting in expedited reconstruction processes, e.g., simultaneous ART[41] and Landweber.[42] Due to the inherent ill-posed nature of inverse problems, regularization techniques are commonly employed. In CFV techniques, two predominant forms of regularization are utilized: Tikhonov regularization,[43] which emphasizes smoothness, and total variation regularization,[31] which balances smoothness with the preservation of sharp edges. In plenoptic imaging, the reconstruction process bears similarities to that of tomography, with the multiplicative ART being the most prevalent method employed for reconstruction[39] because of its fast convergence. The imaging model of digital holography is quite different from tomography and plenoptic imaging, leading to different reconstruction methods.[18,44] The undistorted real image of the target object can be received by illuminating the hologram with the complex conjugate of the reference wave ($E^* R(x,y)$). By back-propagating the light wave ($E^* R(x,y)h(x,y)$) to a specific plane, the image of the object can be reconstructed via Fourier transform such as the angular spectrum algorithm.[18]

In recent years, data-based reconstruction methods have gained increasing popularity due to their rapid reconstruction speed and high level of accuracy.[34,45] The most notable distinction between model-based and data-based reconstruction lies in the fact that data-based approaches require large-scale datasets instead of explicit imaging models. In data-based reconstruction, artificial neural networks play a crucial role in extracting implicit features from the dataset. They have a different architecture[46,47] and have been successfully applied in CFV.[15,18,48] During the supervised training process, the network's output is compared to the labels using a loss function, and the network parameters can be updated iteratively until the loss function converges to a satisfactory level. After training, the network can be deployed for reconstruction purposes. The inputs to the network are typically projections or holograms,[45] while the outputs are the reconstructed images. However, collecting such a large-scale dataset remains a challenge.

Visualization setup

This section summarizes the general visualization setup components for CFV (Figures 1D–1I), including light sources, optical elements, and detectors. More advanced components will be provided in the opportunities section.

Depending on whether an external light source is utilized, CFV can be categorized into passive and active techniques. In active techniques, various light sources have been employed to facilitate the visualization process. The light emitted from the light source passes through the target flow, where it undergoes attenuation,[20] scattering,[39] or deviation[32] or may even excite new light phenomena[6] due to interactions with the flow. Finally, the light that encodes flow information can be recorded by the detector. The laser stands out as the most well-known light source, extensively utilized in tomography, plenoptic imaging, and digital holography. Tailored to specific applications, laser wavelengths span across the ultraviolet, visible, and infrared ranges, with frequencies varying from continuous to high-frequency pulses. Additionally, high-power light-emitting diodes have been introduced in techniques such as BOS tomography and tomographic PIV. Broadband light sources, such as laser-driven light sources and halogen lamps, are typically used when monochromaticity is not a critical requirement or multiple-wavelength illumination is necessary.

In a CFV setup, various optical elements are employed. Among these, the most common is the lens system, which reshapes light and focuses the object onto a detector. Moreover, by using two convex lenses, a 4f system can be established to work as a spatial filter. Prisms and mirrors alter the direction of the light and can sometimes be integrated to form a quadscope. Filters are typically installed in front of detectors to suppress undesired light and transmit desired light, while a polarizer can select the polarization of transmitting light. Attenuators reduce the energy of laser pulses, ensuring that the fluence remains below the damage threshold of other optical components. Beam splitters separate light beams based on specific wavelengths. Gratings are commonly used in spectrometers to disperse light. Diffusers generate uniform illumination and can also alter the profile of a laser beam. Windows are associated with target flow and provide optical access in confinement situations.

For tomography, multiple detectors are positioned around the target flow to capture data from various angles. In contrast, plenoptic imaging and digital holography typically utilize a single detector. Camera specifications for CFV, including sensor size, frame rate, and spectral response, can vary widely. More pixels may provide higher-resolution images, while higher frame rates allow for the capture of fast-flowing phenomena. Spectral response refers to the range of wavelengths that the sensor can detect, which may be important for capturing specific flow phenomena or using specialized lighting sources. In situations where short exposure times and high speed are not critical, lower-cost industrial cameras are often used.[49] However, in situations where high-speed visualization is required to capture fast-moving phenomena,[50] such as in scientific research or high-speed imaging applications, specialized high-speed scientific cameras are necessary. Similarly, in scenarios where the signal strength is low and requires amplification for better imaging, intensified scientific cameras are utilized. These cameras incorporate specialized components such as image intensifiers to enhance the signal-to-noise ratio and improve sensitivity, making them ideal for low-light conditions or applications where weak signals need to be detected.

KEY CHALLENGES

CFV technologies hinge upon the utilization of comprehensive optical systems and sophisticated computational methods to decipher intricate optical-flow information.

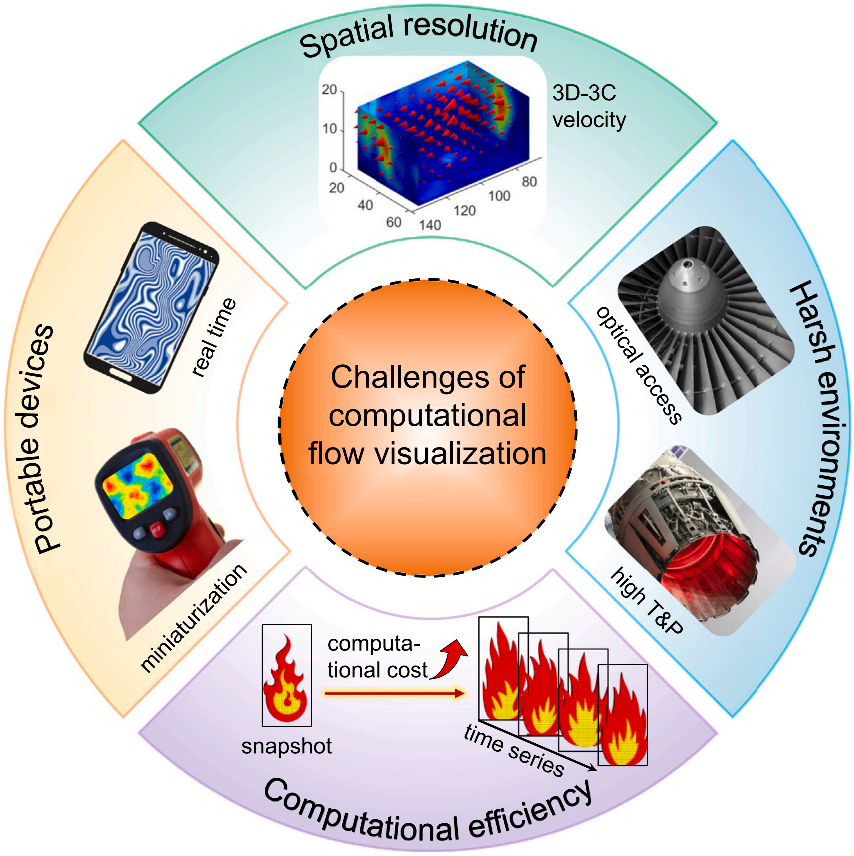

Figure 2. The key challenges of computational flow visualization
The challenges include limited spatial resolution (3D-3C, three-dimensional three-component), limited computational efficiency, lack of robustness in harsh environments (T, temperature; P, pressure), and lack of compact and portable devices.

Consequently, this enables the multi-dimensional and multi-parameters characteristics of the target complex flows to be revealed. Despite its remarkable performance having been demonstrated in various research facilities, the field still encounters numerous hurdles that impede its progression and hinder its practical implementation. The key challenges of CFV (Figure 2) are categorized into limited spatial resolution, limited computational efficiency, lack of robustness in harsh environments, and lack of compact and portable devices. It is noted that these challenges may occur interdependently in specific scenarios. For enhanced clarity, in this section, comprehensive assessment and discussion of these challenges are conducted separately.

Limited spatial resolution

Limited 3D spatial resolution is one of the key challenges in CFV techniques, especially in the axial direction (i.e., perpendicular to the imaging plane) for plenoptic imaging and digital holography.[51] The main reasons for this limitation include spatial sampling rate, optical diffraction, noise, and reconstruction algorithms. Firstly, the spatial resolution of an imaging system is fundamentally limited by the sampling rate, which is dominantly determined by the number of detector elements or pixels in the sensor (typically ranging from 1 to 40 megapixels with micron-level pixel size). If the sampling rate is less than twice the highest spatial frequency (Nyquist-Shannon sampling theorem), then it can lead to aliasing artifacts and a loss of high spatial frequency information in the reconstructed image. Specifically, in tomography, the projection number and angle, which are usually cost related or scenario constrained, can also affect sampling efficiency.[38] Moreover, plenoptic imaging usually has lower spatial resolution due to the finite size of the micro-lenses, their spacing, and angle disparity.[52] Secondly, diffraction sets another fundamental limit on the spatial resolution of an imaging system. The diffraction limit depends on the wavelength of light and the numerical aperture of the imaging system, which is related to the size of the aperture or the focusing angle of the lens.[53] Diffraction effects can cause blurring and limit the ability to resolve fine details in the image. Thirdly, noise, such as electronic noise and photon shot noise, can degrade the spatial resolution of an imaging system.[54] High levels of noise can make it difficult to distinguish small variations in intensity or phase, leading to a loss of fine detail in the reconstructed image. Lastly, the selection of the reconstruction algorithm can also impact the spatial resolution.[55] Some algorithms may be more sensitive to noise or may introduce artifacts that limit the effective spatial resolution. For example, in holographic particle imaging, autofocusing algorithms will directly affect the accuracy of particle positioning and tracking.[56,57]

Limited computational efficiency

To effectively visualize complex, unsteady flow fields in practical applications, computational efficiency remains a significant challenge for CFV techniques. While snapshot flow visualization technologies can provide some instantaneous characteristics of the target flow, researchers continue to pursue advanced techniques with high temporal resolution (e.g., more than 100,000 frames per second) and 3D visualization.[58,59] The extensive amount of raw data generated in CFV techniques (e.g., typically several gigabytes per second for high-speed imaging) presents considerable challenges in terms of data storage, transmission, and processing, leading to significant information redundancy and low computational efficiency.[60] The information redundancy often arises from duplicate recordings of non-interest areas or abundant background elements. For instance, model-based reconstruction algorithms in tomographic imaging typically require tens or hundreds of seconds to process a single frame and repeat for all frames separately (parallel computing can be applied, but more computational resources are required).[15] Although numerous data-based reconstruction algorithms claim to dramatically reduce the reconstruction time (e.g., down to milliseconds),[61,62] data pre-processing and model training remain time consuming (e.g., several hours or more). Furthermore, when faced with different application scenarios, the trained model often cannot be applied directly, necessitating careful adjustments or retraining to achieve optimal reconstruction quality. Due to limited computational efficiency, most existing CFV technologies rely on online data collection and offline processing. To accomplish real-time 3D flow visualization and, consequently, more precise flow field control, it is crucial to urgently address the challenge of improving computational efficiency.

Lack of robustness in harsh environments

The demanding conditions present in various harsh environments pose significant challenges to flow visualization techniques, which are crucial for understanding complex flow dynamics. When examining the intricate characteristics of diverse flow fields, including those found in practical apparatus (e.g., engines, combustors, and wind tunnels), these methodologies often confront substantial interference arising from extreme environments. Such environments are characterized by factors such as mechanical vibration, elevated temperature, high pressure, large density variation, intense turbulence, rapid spatiotemporal dynamics, multiple mixed phases, and multiple scattering events.[63,64] These factors, in turn, contribute to the degradation of raw image quality through motion blur, artifacts, overexposure, and a low signal-to-noise ratio (i.e., below 10 dB), ultimately impacting the final reconstruction accuracy. For example, holographic imaging often encounters challenges related to phase distortion when employed in extreme conditions characterized by the presence of shockwaves and substantial thermal gradients.[65] Furthermore, the confined spaces within which these flow fields exist frequently make it challenging to provide adequate optical detection windows, potentially affecting the robustness and reliability of current flow visualization technologies.[66] For instance, tomographic imaging typically necessitates capturing multiple projections (e.g., more than three) of the target flow field from unique perspectives.[49,67] The restricted optical access and spatial occlusion resulting from intricate channel structures pose pressing issues that need to be solved for this particular volumetric imaging technique to be successfully implemented.

Lack of compact and portable devices

Developing compact and portable devices (i.e., decimeter-level dimensions and kilogram-level weight or less) for *in situ* flow visualization is another important concern. Although laboratory-based flow visualization systems demonstrate impressive performance, the miniaturization of these systems is imperative for numerous applications where space, mobility, and ease of deployment are critical considerations.[68,69] However, achieving compactness and portability while preserving the required functionality and performance is intricate and multifaceted. To attain advanced capabilities in light-field encoding and decoding, CFV systems often necessitate a complex integration of optical elements, sensors, data processing units, and power sources. Shrinking these components without compromising their functionality and performance is a delicate balance. It involves addressing issues such as size constraints, power consumption, heat dissipation, and mechanical stability. For example, the design and fabrication of miniaturized optical systems require precise alignment, packaging, and calibration techniques.[70,71] While minimizing the device's dimensions is advantageous, it may impede the field of view and resolution of flow measurements.[72] Achieving high spatial and temporal resolution in a compact device can be much more challenging due to the limitations imposed by the size of optical components, power supply unit, sensors, and data processing capabilities. In addition, the issues related to data storage, transmission, and user interface must be considered. Efficient data handling and real-time visualization of flow information pose technical hurdles in resource-limited devices. Optimization of reconstruction algorithms, wireless communication protocols, and user-friendly interfaces are essential to accommodate the device's compact nature while still providing meaningful and accessible data representation to users.

OPPORTUNITIES

Owing to its exceptional capability in interpreting light-related flow information, CFV has garnered extensive attention and experienced rapid advancements in recent years. Despite the existing challenges, our optimism regarding this promising paradigm remains steadfast, driven by the inspiring progress at the intersection of material science, optical technologies, and computational science. From the perspective of system optimization, the exploration of novel reconstruction algorithms, imaging modalities, and optical components presents a wealth of opportunities to tackle the aforementioned challenges (Figure 3). This section aims to provide a comprehensive and systematic review of several noteworthy emerging technologies that exhibit substantial potential in augmenting and streamlining CFV techniques.

CellPress
OPEN ACCESS

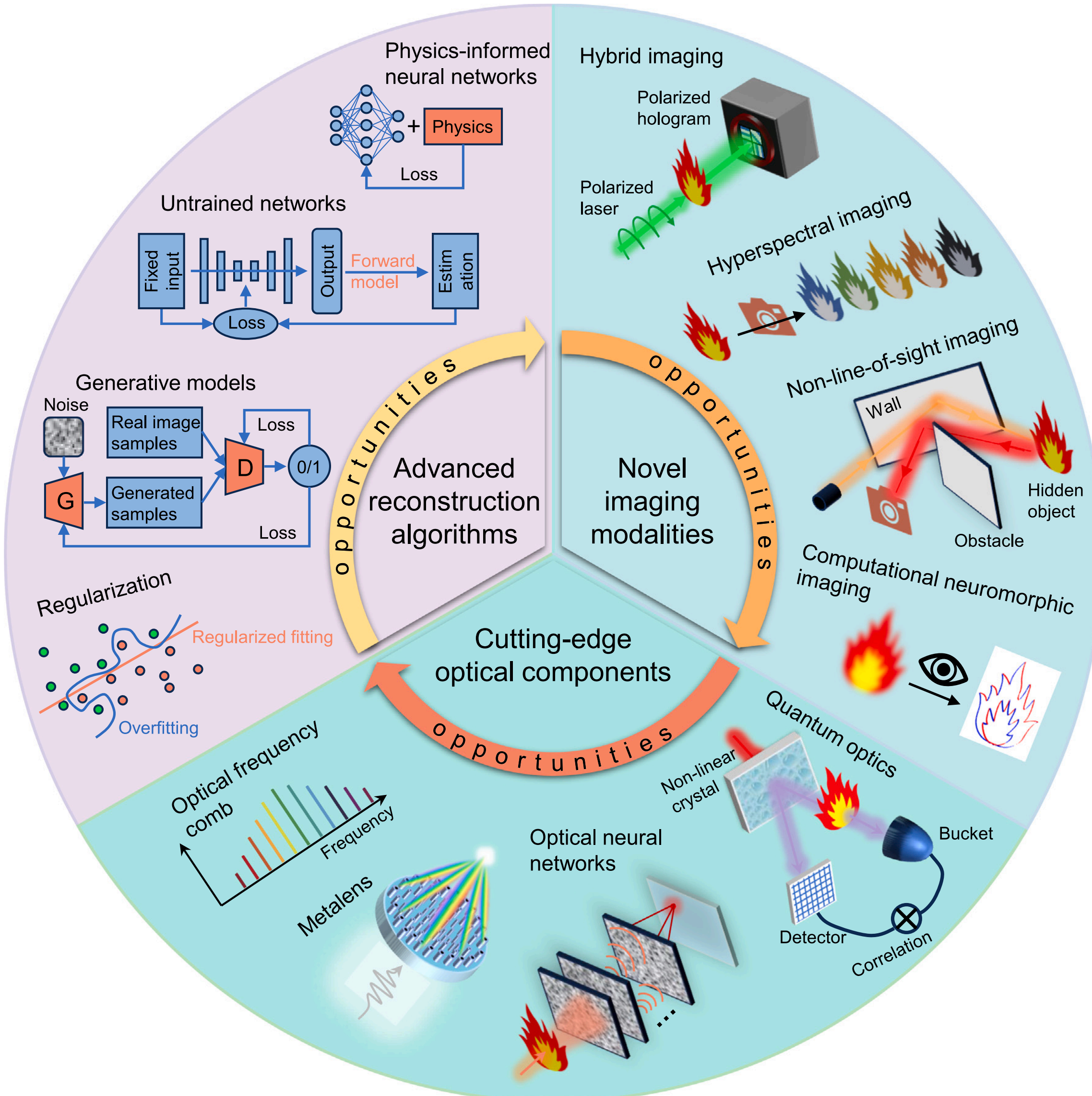

Figure 3. The remarkable opportunities of computational flow visualization

The opportunities are categorized into advanced reconstruction algorithms (including physics-informed neural networks, untrained networks, generative models, and advanced regularization techniques), novel imaging modalities (including hybrid imaging, hyperspectral imaging, non-line-of-sight imaging, and computational neuromorphic imaging), and cutting-edge optical components (including optical frequency comb, metalens, optical neural networks, and quantum optics).

Advanced reconstruction algorithms

When a flow visualization system is well established or a substantial amount of experimental data has already been collected, optimizing the computational methods for the inverse problem becomes a highly effective approach. By leveraging advanced reconstruction algorithms, significant opportunities arise for improving computational efficiency and enhancing the quality of flow reconstruction. We present here several notable techniques that have demonstrated promising results.

PINNs

Physics-informed neural networks (PINNs) integrate domain-specific knowledge and physical principles into neural network architectures, thereby combining the advantages of both model-based and data-based reconstruction techniques.[73] By incorporating governing equations (e.g., Navier-Stokes equations) and boundary conditions as constraints, PINNs can leverage the power of deep learning to infer flow characteristics from sparse or noisy data.[1,74] For example, Wang et al.[75] used a PINN to improve the 3D velocity resolution and predict the pressure field from sparse tomographic PIV data. Cai et al.[76] proposed a PINN-based method to infer 3D velocity and pressure fields from temperature fields provided by BOS tomography. The embedded prior knowledge alleviates the need for large-scale training data and improves the network's interpretability. This approach not only enhances the precision and robustness of solving the inverse problem of flow reconstruction[77] but also enables the extraction of additional physical insights, leading to a more comprehensive understanding of complex flow phenomena.[78]

Untrained networks

Untrained networks, also known as training-free or self-supervised iterative optimization methods, offer an alternative reconstruction approach to CFV. Instead of relying on explicit training (e.g., traditional end-to-end networks[79] typically require supervised training with large-scale, diverse, and labeled data), untrained networks utilize a deep image prior framework[80] to directly reconstruct high-quality flow images from observed data. For instance, Chen et al.[81] demonstrated an untrained U-Net architecture to solve the inverse problem of linear tomographic absorption spectroscopy. Qayyum et al.[82] provided a comprehensive review of untrained networks for various inverse imaging problems such as image restoration, inpainting, and super-resolution. In these paradigms, a known forward-mapping function that represents that the imaging process is embedded in the network for converging the iterative optimization problem, providing enhanced practical interpretability and generalization capabilities.[83] These networks can capture complex relationships and patterns without the need for extensive training datasets, making them particularly useful in scenarios where data collection and annotation are challenging or limited.

Generative models

Generative models, such as generative adversarial networks, variational autoencoders, and probabilistic or score-based diffusion models, offer another powerful framework for solving inverse problems in CFV.[84] Based on an unsupervised learning strategy (without labels), these models can learn the underlying data distribution to solve ill-posed inverse imaging problems, such as limited-projection tomography[85] and single-shot holography.[86] In addition, generative models can leverage the relevant physical laws and constraints to generate synthetic samples that closely resemble real flow visualization data.[87] The captured prior data distribution along with well-established physical models are beneficial for improving the generalization capability of generative models to unknown measurement processes. Generative models enable data augmentation and uncertainty quantification, thereby enhancing the training process and enriching the available data for CFV applications.

Advanced regularization techniques

Advanced regularization techniques play a crucial role in mitigating the ill-posedness and noise sensitivity of flow reconstruction problems, improving the generalization ability of a model.[88] By incorporating prior knowledge or assumptions about the flow field (e.g., similarity, sparsity, smoothness, and symmetry) through regularization terms, these techniques stabilize the inversion process and improve the robustness and accuracy of CFV.[89] By integrating them into the Bayesian framework,[15] it is easy to add more than one kind of regularization and derive uncertainty quantification. Recent research shows that proper modified regularization techniques can further improve the reconstruction accuracy. For example, Cai et al.[90,91] developed several regularization methods for linear/non-linear laser absorption tomography, demonstrating superior reconstruction accuracy of temperature and concentration fields. Cao et al.[92,93] conducted a comprehensive investigation into the utilization of the total variation regularization method in compressive holography, yielding remarkable twin-image suppression in holographic phase and amplitude reconstruction. Regularization methods can effectively suppress artifacts, enhance spatial and temporal resolution, and promote more realistic and physically plausible flow representations.

Novel imaging modalities

The development of novel imaging modalities can indeed lead to fundamental improvements in capturing and interpreting light-related flow information. By pushing the boundaries of imaging techniques, researchers can enhance their ability to capture and analyze flow phenomena based on light interactions. Some remarkable novel imaging modalities are highlighted in this context.

Hybrid imaging

Hybrid imaging, which involves integrating multiple imaging techniques into a single system, offers a versatile strategy for flow visualization.[18] A prime example of this is digital holography,[94] which possesses a simple optical configuration and can be effectively combined with various imaging modalities such as tomographic imaging,[95] scattering imaging,[96] polarization imaging,[97] and two-color imaging pyrometry.[98] On the one hand, hybrid imaging leverages the complementary strengths of different techniques to improve measurement accuracy. For instance, tomographic holography offers a precise method for determining the depth of particles within a volume, circumventing the depth-of-focus limitations encountered in traditional holographic imaging. By integrating multiple imaging techniques, the limitations or errors inherent in one technique can be mitigated or compensated for by the strengths of another. This results in enhanced accuracy and reliability in flow measurements, enabling a more precise understanding of flow behavior and the analysis of flow properties. On the other hand, hybrid imaging enables the detection of a broader range of flow information by combining the capabilities of different imaging modalities. Each technique excels at capturing specific aspects of the flow, such as density gradients, temperature variations, species concentrations, or velocity fields. This simultaneous acquisition of multi-dimensional data enhances the understanding of complex flow behavior and reveals correlations and interactions between different flow parameters.[99]

Hyperspectral imaging

Hyperspectral imaging captures data across a broad range of wavelengths, offering comprehensive spectral information about the reactive flows. Unlike traditional imaging, which captures only a few spectral bands or a single wavelength, hyperspectral imaging enables the discrimination of subtle spectral differences.[100,101] This capability is particularly useful in reactive flow visualization applications where different flow constituents or materials exhibit distinct spectral reflectance or absorption properties. By analyzing the spectral information, researchers can identify and differentiate various components within inhomogeneous or reactive flows,[102] such as different fluids, particles, bubbles, or chemical species. Moreover, hyperspectral imaging can reveal fine details and subtle variations in the flow field with higher spectral resolution. This enhanced contrast and sensitivity enables the detection and visualization of weak or low-contrast flow features that may be challenging to capture using traditional imaging methods. Lastly, by calibrating the hyperspectral system and employing appropriate spectral models, researchers can convert spectral information into quantitative measurements such as concentration, temperature, or velocity.[103] This quantitative analysis provides valuable data for scientific research, engineering applications, and process monitoring, allowing for precise characterization and measurement of flow parameters.

NLOS

Vast amounts of practical scenes for flow visualization are complex in tightly confined spaces or highly indirect around corners, e.g., gas leakage localization inside the pipe and inspection defects inside running aircraft engines. Therefore, there is an urgent demand for flow visualization approaches under such highly ill-posed inverse imaging scenes that can work outside of the direct line-of-sight. Non-line-of-sight (NLOS) imaging is an emerging technique that can detect hidden target information through opaque scattering layers, around corners, or behind other obstacles.[104] To achieve indirect flow detection, more efficient sensing approaches could be introduced into NLOS flow visualization, e.g., high-speed imaging and low redundant tracking.[105,106] NLOS imaging is a feasible and promising technique for signal detection in invisible space and indirect scenes, which will promote unprecedented flow visualization capabilities.

CNI

Event cameras encode per-pixel brightness changes of dynamic scenes with asynchronous events, posing a neuromorphic imaging modal shift against traditional modalities. Equipped with such a new imaging paradigm, event cameras are capable of efficiently handling large-scale visual data with high temporal resolution,[107] high dynamic range, high pixel bandwidth, and minimal data redundancy, among other remarkable features. The convergence of neuromorphic engineering and computational imaging has propelled the rapid growth and advancement of the field of computational neuromorphic imaging (CNI).[108] Recently, BOS with an event camera has been explored for flow visualization,[109,110] and impressive results have been achieved via multimodal fusion within the CNI framework. For instance, Wang et al.[111] proposed neuromorphic Shack-Hartmann wave normal sensing and demonstrated its feasibility in measuring a dynamic flame front. It also has the potential to visualize the flow in low light levels, as the weak optical signals can be detected in logarithmic responses with a higher sensitivity. Therefore, the performance of flow visualization can be efficiently enhanced with the CNI paradigm, which promotes the visualization technique beyond the bandwidth limitation of conventional imaging sensors.

Cutting-edge optical components

Optical components play a critical role in CFV. They are involved in the generation, transmission, manipulation, and detection of light, offering flexibility to capture comprehensive information about the flow. Beyond traditional components in the section of visualization setup, here are several cutting-edge optical components that have the potential to significantly advance CFV, pushing the boundaries of our understanding and control of fluid behavior.

Optical frequency comb

An optical frequency comb[112] is a spectrum of equally spaced frequency lines, representing precise marks in frequency as an optical ruler. Recent advancements in on-chip micro-combs have greatly facilitated the miniaturization and application of this technology. The utilization of an optical frequency comb empowers researchers to explore molecular systems using a diverse array of accurate and precise optical frequencies. It can be used for high-precision measurements of flow properties, such as velocity, temperature, and species concentration, by utilizing techniques like dual-comb spectroscopy. For instance, Schroeder et al.[113] demonstrated the simultaneous measurement of temperature and H_2O and CO_2 concentrations in the exhaust of a gas turbine using dual-frequency comb laser absorption spectroscopy. In addition, it is feasible to integrate optical frequency combs into hyperspectral imaging, holography,[114] and optical coherence tomography,[115] leading to more accurate and high-resolution flow visualization.

Metalens

Metalenses are ultra-thin optical components capable of manipulating light at subwavelength scales.[116] They offer a pathway to create compact, lightweight, and efficient optical systems for flow visualization. For instance, Liu et al.[117] demonstrated a binocular metalens PIV system to resolve 3D velocity fields of vortex rings. In their experiments, the traditional bulky lens system was replaced by a metalens weighing only 116 mg. By designing metalens with specific functionalities such as beam steering, filtering, or focusing, it is possible to develop new measurement techniques, simplify experimental setups, or improve imaging quality for flow visualization.[70,118] A representative case is the application of a metalens in hyperspectral imaging,[119,120] which exhibits superior spectral resolution performance with a compact system. Furthermore, the emergence of tunable or re-configurable metalens has garnered significant attention from the computational imaging and flow visualization communities.[121] These metalenses offer enhanced flexibility in light manipulation, enabling sufficient polarization, spectrum, phase, and amplitude modulation through various switching mechanisms, including optical, chemical, electronic, thermal, and mechanical actuation.[122]

ONNs

Optical neural networks (ONNs) leverage light for information transmission, parallel processing, and intelligent computing through optical propagation. The interconnection forms of neurons in ONNs can be categorized into diffraction, interference, coupling, and scattering types.[123] By utilizing photons as carriers of information instead of electrons (without converting optical signals into electrical signals), ONNs offer distinct advantages such as low energy consumption, minimal latency, rapid computation at the speed of light, and high parallelism.[124] Additionally, the physical architecture of ONNs can be designed using metasurfaces,[125,126] thereby enhancing functionality while reducing weight and volume. Considering these factors, ONNs hold significant potential for processing and analyzing flow visualization data in real-time. This capability can facilitate faster and more efficient analysis of intricate flow phenomena, enabling real-time feedback and control in fluid dynamics experiments or simulations.

Quantum optics

Quantum optics explores the interaction of light with atoms and molecules, e.g., harnessing non-linear crystals to generate entangled photons, potentially leading to the development of new flow visualization techniques. For extreme flow visualization conditions, e.g., in low-light environments, it is crucial to consider the quantum nature of light. This is because the presence of photons or shot noise can limit the quality of the detected image.[127] Quantum imaging is a sub-field of quantum optics that leverages quantum correlations, such as quantum entanglement of the electromagnetic field, to produce advanced imaging techniques for object reconstruction. It promises improved resolution and sensitivity at ultra-low light levels and measurements in extreme noise conditions.[128] Consequently, quantum imaging can serve as a potential tool for sensing the flow of transparent media with weak signals. Moreover, quantum imaging offers a viable method for ensuring precision in flow measurements.[129]

FUTURE RESEARCH DIRECTIONS AND BROADER IMPLICATIONS

As a versatile and powerful technique, CFV enhances the understanding of complex flow systems and supports a wide range of applications. It is important to highlight that the aforementioned three aspects of opportunities are not mutually exclusive but rather can be integrated and coexist harmoniously. With comprehensive consideration of these opportunities, specific promising directions can be explored to further improve flow visualization.

Multi-parameters visualization: instead of focusing on a single flow parameter, such as velocity or temperature, there is potential in visualizing multiple parameters simultaneously. By employing advanced imaging modalities or utilizing multi-functional optical components, researchers can visualize and analyze multiple parameters, such as velocity, temperature, pressure, and species concentration, simultaneously.[32,98,130] This multi-parameter visualization provides a more comprehensive understanding of complex flows and their interactions.[131]

Real-time visualization: real-time flow visualization is crucial for dynamic systems where immediate feedback is required. To achieve this, lightweight computing models and high-efficiency algorithms can be developed to process and analyze the large amount of data generated by imaging techniques.[46,132] Utilizing parallel and distributed computing techniques can further enhance the speed and efficiency of real-time flow visualization, enabling faster decision-making and responsive control in various applications.[133] Moreover, integrated and portable devices are highly desired for flow visualization in different industrial scenarios.

Intelligent flow diagnostics: by incorporating machine learning and artificial intelligence techniques, flow visualization can be enhanced with intelligent flow diagnostics. Classification, recognition, and identification algorithms can be employed to automatically identify and characterize flow patterns, anomalies, or specific flow features of interest.[134,135] This can help researchers and engineers gain insights into flow behavior, detect critical events, and facilitate automated monitoring and control systems. Besides, as a widely recognized mathematical protocol, the data assimilation[136–139] technique can adeptly integrate partial measurements with numerical modeling, yielding enhanced accuracy in flow reconstruction, prediction, and diagnosis.

Beyond common flows like air and water, CFV techniques also have great opportunities for broader applications in various fields, such as oceanography, environmental monitoring, biomedical research, and meteorology. For example, in oceanography, hyperspectral imaging can be used to study the distribution of phytoplankton and pollutants in marine environments.[140] In biomedical research, flow visualization techniques can aid in studying blood flow patterns,[141] drug delivery,[142] and tissue perfusion.[143] By exploring these broader applications, flow visualization can contribute to advancements in multiple scientific disciplines and address specific challenges in different domains.

CONCLUSIONS

In this perspective, we have presented the concept of CFV as a means to achieve higher-resolution, more accurate, and real-time measurements of fluid dynamics and flow phenomena. CFV offers a significant departure from traditional approaches by leveraging comprehensive optical and computational methods to reveal a wealth of information about the flow. We have introduced representative CFV techniques, such as tomography, plenoptic imaging, and digital holography, to illustrate their underlying principles and advantages. These techniques showcase the potential of CFV in capturing detailed flow characteristics and providing valuable insights into complex fluid dynamics. In addition, we have systematically analyzed and categorized the key challenges associated with CFV. These challenges encompass spatial resolution, computational efficiency, harsh environments, and the need for portable devices. However, we are optimistic about the opportunities that lie ahead, driven by the rapid advancements in computer science, optical technologies, and materials science. Specifically, we highlight the promising prospects in terms of advanced reconstruction algorithms, novel imaging modalities, and cutting-edge optical components. By embracing emerging optical and computational approaches, we can overcome existing challenges and pave the way for exciting new discoveries in flow visualization. We anticipate that the fusion of optical and computational techniques will drive the sustainable development of CFV and unlock its full potential in various scientific and engineering domains.

ACKNOWLEDGMENTS

This work is partly funded by the Research Grants Council of Hong Kong (GRF 17201822), the Hong Kong Scholars Program (XJ2022032), and the Alexander von Humboldt Foundation. J.H. and H.L. appreciate the support from Shanghai Jiao Tong University.

AUTHOR CONTRIBUTIONS

J.H. and H.L. wrote the manuscript primarily and prepared figures. S.Z. helped analyze the literature and wrote the manuscript. W.C., E.Y.L., and Y.L. reviewed and edited the manuscript. W.C. and E.Y.L. contributed to funding acquisition and supervised the research and writing of the manuscript.

DECLARATION OF INTERESTS

The authors declare no competing interests.

REFERENCES

1. Raissi, M., Yazdani, A., and Karniadakis, G.E. (2020). Hidden fluid mechanics: Learning velocity and pressure fields from flow visualizations. Science *367*, 1026–1030. https://doi.org/10.1126/science.aaw4741.
2. Merzkirch, W. (2012). Flow Visualization (Elsevier).
3. Adrian, R.J., and Westerweel, J. (2011). Particle Image Velocimetry (Cambridge university press).
4. Hariharan, P. (2010). Basics of Interferometry (Elsevier).
5. Settles, G.S., and Hargather, M.J. (2017). A review of recent developments in schlieren and shadowgraph techniques. Meas. Sci. Technol. *28*, 042001. https://doi.org/10.1088/1361-6501/aa5748.
6. Eghtesad, A., Bijarchi, M.A., Shafii, M.B., and Afshin, H. (2024). A state-of-the-art review on laser-induced fluorescence (lif) method with application in temperature measurement. Int. J. Therm. Sci. *196*, 108686. https://doi.org/10.1016/j.ijthermalsci.2023.108686.
7. Suo, J., Zhang, W., Gong, J., Yuan, X., Brady, D.J., and Dai, Q. (2023). Computational imaging and artificial intelligence: The next revolution of mobile vision. Proc. IEEE *111*, 1607–1639. https://doi.org/10.1109/JPROC.2023.3338272.
8. Liu, J., Feng, Y., Wang, Y., Liu, J., Zhou, F., Xiang, W., Zhang, Y., Yang, H., Cai, C., Liu, F., and Shao, X. (2024). Future-proof imaging: computational imaging. Adv. Imag. *1*, 012001. https://doi.org/10.3788/AI.2024.20003.
9. He, C., Shen, Y., and Forbes, A. (2022). Towards higher-dimensional structured light. Light Sci. Appl. *11*, 205. https://doi.org/10.1038/s41377-022-00897-3.
10. Xiang, M., Liu, F., Liu, J., Dong, X., Liu, Q., and Shao, X. (2024). Computational optical imaging: challenges, opportunities, new trends, and emerging applications. Front. Imaging *3*, 1336829. https://doi.org/10.3389/fimag.2024.1336829.
11. Boominathan, V., Robinson, J.T., Waller, L., and Veeraraghavan, A. (2022). Recent advances in lensless imaging. Optica *9*, 1–16. https://doi.org/10.1364/OPTICA.431361.
12. Yoon, S., Kim, M., Jang, M., Choi, Y., Choi, W., Kang, S., and Choi, W. (2020). Deep optical imaging within complex scattering media. Nat. Rev. Phys. *2*, 141–158. https://doi.org/10.1038/s42254-019-0143-2.
13. Li, X., Han, Y., Wang, H., Liu, T., Chen, S.-C., and Hu, H. (2022). Polarimetric imaging through scattering media: A review. Front. Physiol. *10*, 815296. https://doi.org/10.3389/fphy.2022.815296.
14. Lemos, G.B., Borish, V., Cole, G.D., Ramelow, S., Lapkiewicz, R., and Zeilinger, A. (2014). Quantum imaging with undetected photons. Nature *512*, 409–412. https://doi.org/10.1038/nature13586.
15. Grauer, S.J., Mohri, K., Yu, T., Liu, H., and Cai, W. (2023). Volumetric emission tomography for combustion processes. Prog. Energy Combust. Sci. *94*, 101024. https://doi.org/10.1016/j.pecs.2022.101024.
16. Tan, Z.P., and Thurow, B.S. (2021). Perspective on the development and application of light-field cameras in flow diagnostics. Meas. Sci. Technol. *32*, 101001. https://doi.org/10.1088/1361-6501/ac026e.
17. Katz, J., and Sheng, J. (2010). Applications of holography in fluid mechanics and particle dynamics. Annu. Rev. Fluid Mech. *42*,

531–555. https://doi.org/10.1146/annurev-fluid-121108-145508.

18. Huang, J., Cai, W., Wu, Y., and Wu, X. (2021). Recent advances and applications of digital holography in multiphase reactive/nonreactive flows: a review. Meas. Sci. Technol. *33*, 022001. https://doi.org/10.1088/1361-6501/ac32ea.

19. Memmolo, P., Miccio, L., Paturzo, M., Caprio, G.D., Coppola, G., Netti, P.A., and Ferraro, P. (2015). Recent advances in holographic 3d particle tracking. Adv. Opt. Photonics *7*, 713–755. https://doi.org/10.1364/AOP.7.000713.

20. Wei, C., Schwarm, K.K., Pineda, D.I., and Spearrin, R.M. (2021). Volumetric laser absorption imaging of temperature, co and co2 in laminar flames using 3d masked tikhonov regularization. Combust. Flame *224*, 239–247. https://doi.org/10.1016/j.combustflame.2020.10.031.

21. Peng, F., Liu, H., Zhao, Q., Worth, N., and Cai, W. (2022). Assessment of imaging models for volumetric tomography of fluid flows. Measurement *204*, 112174. https://doi.org/10.1016/j.measurement.2022.112174.

22. Yu, T., Liu, H., and Cai, W. (2017). On the quantification of spatial resolution for threedimensional computed tomography of chemiluminescence. Opt Express *25*, 24093–24108. https://doi.org/10.1364/OE.25.024093.

23. Floyd, J., and Kempf, A. (2011). Computed tomography of chemiluminescence (ctc): High resolution and instantaneous 3-d measurements of a matrix burner. Proc. Combust. Inst. *33*, 751–758. https://doi.org/10.1016/j.proci.2010.06.015.

24. Liu, H., Peng, F., and Cai, W. (2023). A reconstruction method for volumetric tomography within two parallel transparent plates. Opt Laser. Eng. *169*, 107699. https://doi.org/10.1016/j.optlaseng.2023.107699.

25. Scarano, F. (2012). Tomographic piv: principles and practice. Meas. Sci. Technol. *24*, 012001. https://doi.org/10.1088/0957-0233/24/1/012001.

26. Ma, L., Lei, Q., Ikeda, J., Xu, W., Wu, Y., and Carter, C.D. (2017). Single-shot 3d flame diagnostic based on volumetric laser induced fluorescence (vlif). Proc. Combust. Inst. *36*, 4575–4583. https://doi.org/10.1016/j.proci.2016.07.050.

27. Bauer, F.J., Yu, T., Cai, W., Huber, F.J.T., and Will, S. (2021). Three-dimensional particle size determination in a laminar diffusion flame by tomographic laser-induced incandescence. Appl. Phys. B *127*, 4–10. https://doi.org/10.1007/s00340-020-07562-w.

28. Seong, J.H., Song, M.S., Nunez, D., Manera, A., and Kim, E.S. (2019). Velocity refinement of piv using global optical flow. Exp. Fluid *60*, 174. https://doi.org/10.1007/s00348-019-2820-4.

29. Yu, T., Bauer, F.J., Huber, F.J., Will, S., and Cai, W. (2021). 4d temperature measurements using tomographic two-color pyrometry. Opt Express *29*, 5304–5315. https://doi.org/10.1364/OE.412821.

30. Liu, H., Peng, F., Sanders, S.T., and Cai, W. (2023). Laser absorption tomography based on unstructured meshing. Meas. Sci. Technol. *35*, 025201. https://doi.org/10.1088/1361-6501/ad068f.

31. Grauer, S.J., Unterberger, A., Rittler, A., Daun, K.J., Kempf, A.M., and Mohri, K. (2018). Instantaneous 3d flame imaging by background-oriented schlieren tomography. Combust. Flame *196*, 284–299. https://doi.org/10.1016/j.combustflame.2018.06.022.

32. Liu, H., Huang, J., Li, L., and Cai, W. (2021). Volumetric imaging of flame refractive index, density, and temperature using background-oriented schlieren tomography. Sci. China Technol. Sci. *64*, 98–110. https://doi.org/10.1007/s11431-020-1663-5.

33. Lam, E.Y. (2015). Computational photography with plenoptic camera and light field capture: tutorial. J. Opt. Soc. Am. A *32*, 2021–2032. https://doi.org/10.1364/JOSAA.32.002021.

34. Wang, K., Song, L., Wang, C., Ren, Z., Zhao, G., Dou, J., Di, J., Barbastathis, G., Zhou, R., Zhao, J., and Lam, E.Y. (2024). On the use of deep learning for phase recovery. Light Sci. Appl. *13*, 4. https://doi.org/10.1038/s41377-023-01340-x.

35. Raghavan, K., and Yagle, A.E. (1994). Forward and inverse problems in elasticity imaging of soft tissues. IEEE Trans. Nucl. Sci. *41*, 1639–1648. https://doi.org/10.1109/23.322961.

36. Bertero, M., Boccacci, P., and De Mol, C. (2021). Introduction to Inverse Problems in Imaging (CRC press). https://doi.org/10.1201/9780367806941.

37. Dasch, C.J. (1992). One-dimensional tomography: a comparison of abel, onion-peeling, and filtered backprojection methods. Appl. Opt. *31*, 1146–1152. https://doi.org/10.1364/AO.31.001146.

38. Liu, H., Wang, Q., and Cai, W. (2020). Parametric study on single-camera endoscopic tomography. J. Opt. Soc. Am. B *37*, 271–278. https://doi.org/10.1364/JOSAB.379793.

39. Shi, S., Wang, J., Ding, J., Zhao, Z., and New, T. (2016). Parametric study on light field volumetric particle image velocimetry. Flow Meas. Instrum. *49*, 70–88. https://doi.org/10.1016/j.flowmeasinst.2016.05.006.

40. Gaitanis, A., Kontaxakis, G., Spyrou, G., Panayiotakis, G., and Tzanakos, G. (2010). Pet image reconstruction: A stopping rule for the mlem algorithm based on properties of the updating coefficients. Comput. Med. Imag. Graph. *34*, 131–141. https://doi.org/10.1016/j.compmedimag.2009.07.006.

41. Jiang, M., and Wang, G. (2003). Convergence of the simultaneous algebraic reconstruction technique (sart). IEEE Trans. Image Process. *12*, 957–961. https://doi.org/10.1109/TIP.2003.815295.

42. Yang, W.Q., Spink, D.M., York, T.A., and McCann, H. (1999). An image-reconstruction algorithm based on landweber's iteration method for electrical-capacitance tomography. Meas. Sci. Technol. *10*, 1065–1069. https://doi.org/10.1088/0957-0233/10/11/315.

43. Vauhkonen, M., Vadasz, D., Karjalainen, P.A., Somersalo, E., and Kaipio, J.P. (1998). Tikhonov regularization and prior information in electrical impedance tomography. IEEE Trans. Med. Imag. *17*, 285–293. https://doi.org/10.1109/42.700740.

44. Chen, N., Lam, E.Y., Poon, T.-C., and Lee, B. (2020). Sectional hologram reconstruction through complex deconvolution. Opt Laser. Eng. *127*, 105945. https://doi.org/10.1016/j.optlaseng.2019.105945.

45. Zeng, T., Zhu, Y., and Lam, E.Y. (2021). Deep learning for digital holography: a review. Opt Express *29*, 40572–40593. https://doi.org/10.1364/OE.443367.

46. Huang, J., Liu, H., and Cai, W. (2019). Online in situ prediction of 3-d flame evolution from its history 2-d projections via deep learning. J. Fluid Mech. *875*, R2. https://doi.org/10.1017/jfm.2019.545.

47. Deng, A., Huang, J., Liu, H., and Cai, W. (2020). Deep learning algorithms for temperature field reconstruction of nonlinear tomographic absorption spectroscopy. Measurement: Sensors *10–12*, 100024. https://doi.org/10.1016/j.measen.2020.100024.

48. Liu, C., Jiang, R., Wei, D., Yang, C., Li, Y., Wang, F., and Yuan, X. (2022). Deep learning approaches in flow visualization. Adv. Aerodyn. *4*, 17. https://doi.org/10.1186/s42774-022-00113-1.

49. Sanned, D., Lindström, J., Roth, A., Aldén, M., and Richter, M. (2022). Arbitrary position' 3d tomography for practical application in combustion diagnostics. Meas. Sci. Technol. *33*, 125206. https://doi.org/10.1088/1361-6501/ac92a1.

50. Zhao, Y., Wang, L., Zhang, H., Wang, Y., Wu, Y., Wu, X., Wang, G., Song, G., Liu, T., and Zhao, T. (2024). Dual-camera off-axis holographic particle tracking velocimetry: Development and application to air-blast swirl spray measurement. Opt Laser. Eng. *178*, 108237. https://doi.org/10.1016/j.optlaseng.2024.108237.

51. Latychevskaia, T. (2019). Lateral and axial resolution criteria in incoherent and coherent optics and holography, near-and far-field regimes. Appl. Opt. *58*, 3597–3603. https://doi.org/10.1364/AO.58.003597.

52. Deem, E.A., Zhang, Y., Cattafesta, L.N., Fahringer, T.W., and Thurow, B.S. (2016). On the resolution of plenoptic piv. Meas. Sci. Technol. *27*, 084003. https://doi.org/10.1088/0957-0233/27/8/084003.

53. Gao, P., and Yuan, C. (2022). Resolution enhancement of digital holographic microscopy via synthetic aperture: a review. gxjzz. *3*, 105–120. https://doi.org/10.37188/lam.2022.006.

54. Gureyev, T.E., Paganin, D.M., Kozlov, A., Nesterets, Y.I., and Quiney, H.M. (2018). Complementary aspects of spatial resolution and signal-to-noise ratio in computational imaging. Phys. Rev. *97*, 053819. https://doi.org/10.1103/PhysRevA.97.053819.

55. Shui, C., Liu, H., and Cai, W. (2021). Benchmark evaluation of tomographic algorithms for simultaneous reconstruction of

temperature and volume fraction fields of soot and metaloxide nanoparticles in non-uniform flames. Sci. China Technol. Sci. *64*, 237–250. https://doi.org/10.1007/s11431-019-1507-6.

56. Huang, J., Li, S., Zi, Y., Qian, Y., Cai, W., Aldén, M., and Li, Z. (2021). Clustering-based' particle detection method for digital holography to detect the three-dimensional location and in-plane size of particles. Meas. Sci. Technol. *32*, 055205. https://doi.org/10.1088/1361-6501/abd7aa.

57. Ren, Z., Chen, N., and Lam, E.Y. (2017). Automatic focusing for multisectional objects in digital holography using the structure tensor. Opt. Lett. *42*, 1720–1723. https://doi.org/10.1364/OL.42.001720.

58. Buchmann, N.A., Atkinson, C., and Soria, J. (2012). Ultra-high-speed tomographic digital holographic velocimetry in supersonic particle-laden jet flows. Meas. Sci. Technol. *24*, 024005. https://doi.org/10.1088/0957-0233/24/2/024005.

59. Huang, J., Liu, H., Wang, Q., and Cai, W. (2020). Limited-projection volumetric tomography for time-resolved turbulent combustion diagnostics via deep learning. Aero. Sci. Technol. *106*, 106123. https://doi.org/10.1016/j.ast.2020.106123.

60. Niu, Z.-T., Qi, H., Shi, J.-W., Ren, Y.-T., He, M.-J., and Zhou, W. (2022). Threedimensional rapid visualization of flame temperature field via compression and noise reduction of light field imaging. Int. Commun. Heat Mass Tran. *137*, 106270. https://doi.org/10.1016/j.icheatmasstransfer.2022.106270.

61. Huang, J., Liu, H., Dai, J., and Cai, W. (2018). Reconstruction for limited-data nonlinear tomographic absorption spectroscopy via deep learning. J. Quant. Spectrosc. Radiat. Transf. *218*, 187–193. https://doi.org/10.1016/j.jqsrt.2018.07.011.

62. Huang, J., Zhao, J., and Cai, W. (2019). Compressing convolutional neural networks using pod for the reconstruction of nonlinear tomographic absorption spectroscopy. Comput. Phys. Commun. *241*, 33–39. https://doi.org/10.1016/j.cpc.2019.03.020.

63. Perissinotto, R.M., Monte Verde, W., Biazussi, J.L., Bulgarelli, N.A.V., Fonseca, W.D.P., Castro, M.S.d., Franklin, E.d.M., and Bannwart, A.C. (2021). Flow visualization in centrifugal pumps: A review of methods and experimental studies. J. Pet. Sci. Eng. *203*, 108582. https://doi.org/10.1016/j.petrol.2021.108582.

64. Alden, M. (2023). Spatially and temporally resolved laser/optical diagnostics of combustion' processes: From fundamentals to practical applications. Proc. Combust. Inst. *39*, 1185–1228. https://doi.org/10.1016/j.proci.2022.06.020.

65. Marsh, A.W., D'Ambra, Z., McMaster, A., Guildenbecher, D.R., and Mazumdar, Y.C. (2023). Analysis of holography techniques for phase distortion removal in extreme environments. In AIAA SCITECH 2023 Forum, p. 0803. https://doi.org/10.2514/6.2023-0803.

66. Wang, Q., Yu, T., Liu, H., Huang, J., and Cai, W. (2020). Optimization of camera arrangement for volumetric tomography with constrained optical access. J. Opt. Soc. Am. B *37*, 1231–1239. https://doi.org/10.1364/JOSAB.385291.

67. Chen, H., Ling, C., Wu, Y., Gao, Y., and Li, Y. (2024). Cross-interface computed tomography applied in flame propagation detection of an optical engine. Combust. Flame *261*, 113288. https://doi.org/10.1016/j.combustflame.2023.113288.

68. Yang, Z., Albrow-Owen, T., Cai, W., and Hasan, T. (2021). Miniaturization of optical spectrometers. Science *371*, eabe0722. https://doi.org/10.1126/science.abe0722.

69. Nayak, A.R., Malkiel, E., McFarland, M.N., Twardowski, M.S., and Sullivan, J.M. (2021). A review of holography in the aquatic sciences: in situ characterization of particles, plankton, and small scale biophysical interactions. Front. Mar. Sci. *7*, 572147. https://doi.org/10.3389/fmars.2020.572147.

70. Lee, D., Kim, M., and Rho, J. (2021). Next-generation imaging techniques: functional and miniaturized optical lenses based on metamaterials and metasurfaces. Micromachines *12*, 1142. https://doi.org/10.3390/mi12101142.

71. Huang, J., Li, Y., Zhu, Y., and Lam, E.Y. (2024). A field deployable imaging system for detecting microplastics in the aquatic environment. In 2024 IEEE International Symposium on Circuits and Systems (ISCAS), pp. 1–5. https://doi.org/10.1109/ISCAS58744.2024.10557869.

72. Li, B., Piyawattanametha, W., and Qiu, Z. (2019). Metalens-based miniaturized optical systems. Micromachines *10*, 310. https://doi.org/10.3390/mi10050310.

73. Raissi, M., Perdikaris, P., and Karniadakis, G.E. (2019). Physics-informed neural networks: A deep learning framework for solving forward and inverse problems involving nonlinear partial differential equations. J. Comput. Phys. *378*, 686–707. https://doi.org/10.1016/j.jcp.2018.10.045.

74. Mao, Z., Jagtap, A.D., and Karniadakis, G.E. (2020). Physics-informed neural networks for high-speed flows. Comput. Methods Appl. Mech. Eng. *360*, 112789. https://doi.org/10.1016/j.cma.2019.112789.

75. Wang, H., Liu, Y., and Wang, S. (2022). Dense velocity reconstruction from particle image velocimetry/particle tracking velocimetry using a physics-informed neural network. Phys. Fluids *34*, 017116. https://doi.org/10.1063/5.0078143.

76. Cai, S., Wang, Z., Fuest, F., Jeon, Y.J., Gray, C., and Karniadakis, G.E. (2021). Flow over an espresso cup: inferring 3-d velocity and pressure fields from tomographic background oriented schlieren via physics-informed neural networks. J. Fluid Mech. *915*, A102. https://doi.org/10.1017/jfm.2021.135.

77. Wei, C., Schwarm, K.K., Pineda, D.I., and Mitchell Spearrin, R. (2021). Physics-trained neural network for sparse-view volumetric laser absorption imaging of species and temperature in reacting flows. Opt Express *29*, 22553–22566. https://doi.org/10.1364/OE.427730.

78. Cai, S., Mao, Z., Wang, Z., Yin, M., and Karniadakis, G.E. (2021). Physics-informed neural networks (pinns) for fluid mechanics: A review. Acta Mech. Sin. *37*, 1727–1738. https://doi.org/10.1007/s10409-021-01148-1.

79. Ren, Z., Xu, Z., and Lam, E.Y. (2019). End-to-end deep learning framework for digital holographic reconstruction. Adv. Photonics *1*, 1. https://doi.org/10.1117/1.AP.1.1.016004.

80. Ulyanov, D., Vedaldi, A., and Lempitsky, V. (2018). Deep image prior. In Proceedings of the IEEE conference on computer vision and pattern recognition, pp. 9446–9454.

81. Chen, J., Xu, S., Liu, H., Huang, J., Liu, Y., and Cai, W. (2024). Untrained neural network for linear tomographic absorption spectroscopy. Sci. China Technol. Sci. *67*, 2787–2796. https://doi.org/10.1007/s11431-023-2629-2.

82. Qayyum, A., Ilahi, I., Shamshad, F., Boussaid, F., Bennamoun, M., and Qadir, J. (2022). Untrained neural network priors for inverse imaging problems: A survey. IEEE Trans. Pattern Anal. Mach. Intell. *45*, 6511–6520. https://doi.org/10.1109/TPAMI.2022.3204527.

83. Wang, F., Bian, Y., Wang, H., Lyu, M., Pedrini, G., Osten, W., Barbastathis, G., and Situ, G. (2020). Phase imaging with an untrained neural network. Light Sci. Appl. *9*, 77. https://doi.org/10.1038/s41377-020-0302-3.

84. Zhao, Z., Ye, J.C., and Bresler, Y. (2023). Generative models for inverse imaging problems: From mathematical foundations to physics-driven applications. IEEE Signal Process. Mag. *40*, 148–163. https://doi.org/10.1109/MSP.2022.3215282.

85. Song, Y., Shen, L., Xing, L., and Ermon, S. (2021). Solving inverse problems in medical imaging with score-based generative models. Preprint at arXiv. https://doi.org/10.48550/arXiv.2111.08005.

86. Zhang, Y., Liu, X., and Lam, E.Y. (2024). Single-shot inline holography using a physicsaware diffusion model. Opt Express *32*, 10444–10460. https://doi.org/10.1364/OE.517233.

87. Gao, H., Han, X., Fan, X., Sun, L., Liu, L.-P., Duan, L., and Wang, J.-X. (2024). Bayesian conditional diffusion models for versatile spatiotemporal turbulence generation. Comput. Methods Appl. Mech. Eng. *427*, 117023. https://doi.org/10.1016/j.cma.2024.117023.

88. Tian, Y., and Zhang, Y. (2022). A comprehensive survey on regularization strategies in machine learning. Inf. Fusion *80*, 146–166. https://doi.org/10.1016/j.inffus.2021.11.005.

89. Etminan, A., Muzychka, Y.S., Pope, K., and Nyantekyi-Kwakye, B. (2022). Flow visualization: state-of-the-art development of micro-particle image velocimetry. Meas. Sci. Technol. *33*, 092002. https://doi.org/10.1088/1361-6501/ac75b0.

90. Shui, C., Wang, Y., Cai, W., and Zhou, B. (2021). Linear multispectral absorption tomography based on regularized iterative methods. Opt Express *29*, 20889–20912. https://doi.org/10.1364/OE.421817.

91. Dai, J., Yu, T., Xu, L., and Cai, W. (2018). On the regularization for nonlinear tomographic absorption spectroscopy. J. Quant. Spectrosc. Radiat. Transf. *206*, 233–241. https://doi.org/10.1016/j.jqsrt.2017.11.016.

92. Zhang, W., Cao, L., Brady, D.J., Zhang, H., Cang, J., Zhang, H., and Jin, G. (2018). Twinimage-free holography: a compressive sensing approach. Phys. Rev. Lett. *121*, 093902. https://doi.org/10.1103/PhysRevLett.121.093902.

93. Gao, Y., and Cao, L. (2024). Motion-resolved, reference-free holographic imaging via spatiotemporally regularized inversion. Optica *11*, 32–41. https://doi.org/10.1364/OPTICA.506572.

94. Matoba, O., Quan, X., Xia, P., Awatsuji, Y., and Nomura, T. (2017). Multimodal imaging based on digital holography. Proc. IEEE *105*, 906–923. https://doi.org/10.1109/JPROC.2017.2656148.

95. Xia, P., and Ri, S. (2023). Three-dimensional phase measurement of transparent gas by high-speed digital holographic tomography system. Opt Laser. Eng. *168*, 107656. https://doi.org/10.1016/j.optlaseng.2023.107656.

96. Liebel, M., Pazos-Perez, N., van Hulst, N.F., and Alvarez-Puebla, R.A. (2020). Surfaceenhanced raman scattering holography. Nat. Nanotechnol. *15*, 1005–1011. https://doi.org/10.1038/s41565-020-0771-9.

97. Huang, J., Zhu, Y., Li, Y., and Lam, E.Y. (2023). Snapshot polarization-sensitive holography for detecting microplastics in turbid water. ACS Photonics *10*, 4483–4493. https://doi.org/10.1021/acsphotonics.3c01350.

98. Marsh, A.W., Wang, G.T., Heyborne, J.D., Guildenbecher, D.R., and Mazumdar, Y.C. (2021). Time-resolved size, velocity, and temperature statistics of aluminum combustion in solid rocket propellants. Proc. Combust. Inst. *38*, 4417–4424. https://doi.org/10.1016/j.proci.2020.08.010.

99. Foo, C.T., Unterberger, A., Menser, J., and Mohri, K. (2021). Tomographic imaging using multi-simultaneous measurements (times) for flame emission reconstructions. Opt Express *29*, 244–255. https://doi.org/10.1364/OE.412048.

100. Ghamisi, P., Yokoya, N., Li, J., Liao, W., Liu, S., Plaza, J., Rasti, B., and Plaza, A. (2017). Advances in hyperspectral image and signal processing: A comprehensive overview of the state of the art. IEEE Geosci. Remote Sens. Mag. *5*, 37–78. https://doi.org/10.1109/MGRS.2017.2762087.

101. Yuan, L., Song, Q., Liu, H., Heggarty, K., and Cai, W. (2023). Super-resolution computed tomography imaging spectrometry. Photon. Res. *11*, 212–224. https://doi.org/10.1364/PRJ.472072.

102. Si, M., Cheng, Q., Yuan, L., Luo, Z., Yan, W., and Zhou, H. (2021). Study on the combustion behavior and soot formation of single coal particle using hyperspectral imaging technique. Combust. Flame *233*, 111568. https://doi.org/10.1016/j.combustflame.2021.111568.

103. Zheng, S., Cai, W., Sui, R., Luo, Z., and Lu, Q. (2022). In-situ measurements of temperature and emissivity during msw combustion using spectral analysis and multispectral imaging processing. Fuel *323*, 124328. https://doi.org/10.1016/j.fuel.2022.124328.

104. Faccio, D., Velten, A., and Wetzstein, G. (2020). Non-line-of-sight imaging. Nat. Rev. Phys. *2*, 318–327. https://doi.org/10.1038/s42254-020-0174-8.

105. Liu, L., Zhu, S., Zhang, W., Bai, L., Guo, E., and Han, J. (2024). Single-shot non-lineof-sight imaging based on chromato-axial differential correlography. Photon. Res. *12*, 106–114. https://doi.org/10.1364/PRJ.501597.

106. Zhu, S., Ge, Z., Wang, C., Han, J., and Lam, E.Y. (2024). Efficient non-line-of-sight tracking with computational neuromorphic imaging. Opt. Lett. *49*, 3584–3587. https://doi.org/10.1364/OL.530066.

107. Ge, Z., Wei, H., Xu, F., Gao, Y., Chu, Z., So, H.K.-H., and Lam, E.Y. (2023). Millisecond autofocusing microscopy using neuromorphic event sensing. Opt Laser. Eng. *160*, 107247. https://doi.org/10.1016/j.optlaseng.2022.107247.

108. Zhu, S., Wang, C., Liu, H., Zhang, P., and Lam, E.Y. (2024). Computational neuromorphic imaging: principles and applications Computational Optical Imaging and Artificial Intelligence in Biomedical Sciences. SPIEL *12857*, 4–10. https://doi.org/10.1117/12.3012192.

109. Shiba, S., Hamann, F., Aoki, Y., and Gallego, G. (2024). Event-based background-oriented schlieren. IEEE Trans. Pattern Anal. Mach. Intell. *46*, 2011–2026. https://doi.org/10.1109/TPAMI.2023.3328188.

110. Lyu, Z., Cai, W., and Liu, Y. (2024). Event-triggered background-oriented schlieren: highfrequency visualization of a heated jet flow. Opt. Lett. *49*, 2565–2568. https://doi.org/10.1364/OL.515700.

111. Wang, C., Zhu, S., Zhang, P., Huang, J., Wang, K., and Lam, E.Y. (2024). Neuromorphic shack-hartmann wave normal sensing. Preprint at arXiv. https://arxiv.org/abs/2404.15619.

112. Chang, L., Liu, S., and Bowers, J.E. (2022). Integrated optical frequency comb technologies. Nat. Photonics *16*, 95–108. https://doi.org/10.1038/s41566-021-00945-1.

113. Schroeder, P.J., Wright, R.J., Coburn, S., Sodergren, B., Cossel, K.C., Droste, S., Truong, G.W., Baumann, E., Giorgetta, F.R., Coddington, I., et al. (2017). Dual frequency comb laser absorption spectroscopy in a 16 mw gas turbine exhaust. Proc. Combust. Inst. *36*, 4565–4573. https://doi.org/10.1016/j.proci.2016.06.032.

114. Vicentini, E., Wang, Z., Van Gasse, K., Hänsch, T.W., and Picqué, N. (2021). Dual-' comb hyperspectral digital holography. Nat. Photonics *15*, 890–894. https://doi.org/10.1038/s41566-021-00892-x.

115. Ji, X., Yao, X., Klenner, A., Gan, Y., Gaeta, A.L., Hendon, C.P., and Lipson, M. (2019). Chip-based frequency comb sources for optical coherence tomography. Opt Express *27*, 19896–19905. https://doi.org/10.1364/OE.27.019896.

116. Kuznetsov, A.I., Brongersma, M.L., Yao, J., Chen, M.K., Levy, U., Tsai, D.P., Zheludev, N.I., Faraon, A., Arbabi, A., Yu, N., et al. (2024). Roadmap for optical metasurfaces. ACS Photonics *11*, 816–865. https://doi.org/10.1021/acsphotonics.3c00457.

117. Liu, X., Zhao, Z., Xu, S., Zhang, J., Zhou, Y., He, Y., Yamaguchi, T., Ouyang, H., Tanaka, T., Chen, M.K., et al. (2023). Meta-lens particle image velocimetry. Adv. Mater. *36*, 2310134. https://doi.org/10.1002/adma.202310134.

118. Peng, Y., Zhang, J., Zhou, X., Chen, C., Guo, T., Yan, Q., Zhang, Y., and Wu, C. (2024). Metalens in improving imaging quality: advancements, challenges, and prospects for future display. Laser Photon. Rev. *18*, 2300731. https://doi.org/10.1002/lpor.202300731.

119. Hua, X., Wang, Y., Wang, S., Zou, X., Zhou, Y., Li, L., Yan, F., Cao, X., Xiao, S., Tsai, D.P., et al. (2022). Ultra-compact snapshot spectral light-field imaging. Nat. Commun. *13*, 2732.

120. Lin, C.-H., Huang, S.-H., Lin, T.-H., and Wu, P.C. (2023). Metasurface-empowered snapshot hyperspectral imaging with convex/deep (code) small-data learning theory. Nat. Commun. *14*, 6979.

121. Hu, X., Xu, W., Fan, Q., Yue, T., Yan, F., Lu, Y., and Xu, T. (2024). Metasurface-based computational imaging: a review. Adv. Photon. *6*, 014002. https://doi.org/10.1117/1.AP.6.1.014002.

122. Mikheeva, E., Kyrou, C., Bentata, F., Khadir, S., Cueff, S., and Genevet, P. (2022). Space and time modulations of light with metasurfaces: recent progress and future prospects. ACS Photonics *9*, 1458–1482. https://doi.org/10.1021/acsphotonics.1c01833.

123. Chen, H., Lou, S., Wang, Q., Huang, P., Duan, H., and Hu, Y. (2024). Diffractive deep neural networks: Theories, optimization, and applications. Appl. Phys. Rev. *11*, 021332. https://doi.org/10.1063/5.0191977.

124. Wang, T., Ma, S.-Y., Wright, L.G., Onodera, T., Richard, B.C., and McMahon, P.L. (2022). An optical neural network using less than 1 photon per multiplication. Nat. Commun. *13*, 123. https://doi.org/10.1038/s41467-021-27774-8.

125. Luo, X., Hu, Y., Ou, X., Li, X., Lai, J., Liu, N., Cheng, X., Pan, A., and Duan, H. (2022). Metasurface-enabled on-chip multiplexed diffractive neural networks in the visible. Light Sci. Appl. *11*, 158. https://doi.org/10.1038/s41377-022-00844-2.

126. Luo, M., Xu, T., Xiao, S., Tsang, H.K., Shu, C., and Huang, C. (2024). Meta-optics based parallel convolutional processing for neural network accelerator. Laser Photon. Rev. 2300984. https://doi.org/10.1002/lpor.202300984.

127. Zhang, Y., Chan, S.H., and Lam, E.Y. (2023). Photon-starved snapshot holography. APL Photonics *8*, 056106. https://doi.org/10.1063/5.0145833.

128. Altmann, Y., McLaughlin, S., Padgett, M.J., Goyal, V.K., Hero, A.O., and Faccio, D. (2018). Quantum-inspired computational imaging. Science *361*, eaat2298. https://doi.org/10.1126/science.aat2298.

129. Xavier, J., Yu, D., Jones, C., Zossimova, E., and Vollmer, F. (2021). Quantum nanophotonic and nanoplasmonic sensing: towards quantum optical bioscience laboratories on chip. Nanophotonics *10*, 1387–1435. https://doi.org/10.1515/nanoph-2020-0593.

130. Wang, Q., Huang, J., Liu, H., Qin, Z., and Cai, W. (2023). 3d particle sizing, thermometry and velocimetry of combusting aluminized propellants. Combust. Flame *247*, 112500. https://doi.org/10.1016/j.combustflame.2022.112500.

131. Zhou, B., Li, T., Frank, J.H., Dreizler, A., and Böhm, B. (2021). Simultaneous 10 khz̈ three-dimensional ch2o and tomographic piv measurements in a lifted partially-premixed jet flame. Proc. Combust. Inst. *38*, 1675–1683. https://doi.org/10.1016/j.proci.2020.07.039.

132. Wang, Z., Zhu, L., Zhang, H., Li, G., Yi, C., Li, Y., Yang, Y., Ding, Y., Zhen, M., Gao, S., et al. (2021). Real-time volumetric reconstruction of biological dynamics with light-field microscopy and deep learning. Nat. Methods *18*, 551–556. https://doi.org/10.5281/zenodo.4390067.

133. Li, Y., Chang, J., Kong, C., and Bao, W. (2022). Recent progress of machine learning in flow modeling and active flow control. Chin. J. Aeronaut. *35*, 14–44. https://doi.org/10.1016/j.cja.2021.07.027.

134. Wang, Y., Yu, Y., Zhu, X., and Zhang, Z. (2020). Pattern recognition for measuring the flame stability of gas-fired combustion based on the image processing technology. Fuel *270*, 117486. https://doi.org/10.1016/j.fuel.2020.117486.

135. Hassanaly, M., and Raman, V. (2021). Classification and computation of extreme events in turbulent combustion. Prog. Energy Combust. Sci. *87*, 100955. https://doi.org/10.1016/j.pecs.2021.100955.

136. Clark Di Leoni, P., Mazzino, A., and Biferale, L. (2020). Synchronization to big data: Nudging the navier-stokes equations for data assimilation of turbulent flows. Phys. Rev. X *10*, 011023.

137. He, C., Wang, P., Liu, Y., and Gan, L. (2022). Flow enhancement of tomographic particle image velocimetry measurements using sequential data assimilation. Phys. Fluids *34*, 035101.

138. Zhou, K., Grauer, S., Schanz, D., Godbersen, P., Schroder, A., Rockstroh, T., Jeon, Y., and ̀Wieneke, B. (2024). Benchmarking data assimilation algorithms for 3d lagrangian particle tracking. In 21st International Symposium on the Application of Laser and Imaging Techniques to Fluid Mechanics, Lisbon, Portugal, pp. 1–22.

139. Singh, A., Molnar, J.P., Grauer, S., and Sidharth, G. (2022). Aggregate loss data assimilation (alda) for supersonic bos. Bull. Am. Phys. Soc. *67*.

140. Kramer, S.J., Siegel, D.A., Maritorena, S., and Catlett, D. (2022). Modeling surface ocean phytoplankton pigments from hyperspectral remote sensing reflectance on global scales. Remote Sens. Environ. *270*, 112879. https://doi.org/10.1016/j.rse.2021.112879.

141. Miller, D.R., Ashour, R., Sullender, C.T., and Dunn, A.K. (2022). Continuous blood flow visualization with laser speckle contrast imaging during neurovascular surgery. Neurophotonics *9*, 021908. https://doi.org/10.1117/1.NPh.9.2.021908.

142. Jeong, J., Jang, D., Kim, D., Lee, D., and Chung, S.K. (2020). Acoustic bubble-based drug manipulation: Carrying, releasing and penetrating for targeted drug delivery using an electromagnetically actuated microrobot. Sens. Actuator A-Phys. *306*, 111973. https://doi.org/10.1016/j.sna.2020.111973.

143. Heeman, W., Maassen, H., Calon, J., Van Goor, H., Leuvenink, H., van Dam, G.M., and Boerma, E.C. (2021). Real-time visualization of renal microperfusion using laser speckle contrast imaging. J. Biomed. Opt. *26*, 056004. https://doi.org/10.1117/1.JBO.26.5.056004.